

SUPPLEMENTARY INFORMATION

**Electronic Structure Engineering of Tin Telluride through Co-doping of
Bismuth and Indium for High Performance Thermoelectrics: A Synergistic
Effect Leading to Record High Room Temperature ZT in Tin Telluride**

U Sandhya Shenoy^{a#} and D Krishna Bhat^{b*}

^aDepartment of Chemistry, College of Engineering and Technology, Srinivas University, Mukka
Mangalore - 574146, India

^bDepartment of Chemistry, National Institute of Technology Karnataka, Surathkal
Mangalore - 575025, India

Corresponding authors email: *denthajekb@gmail.com #sandhyashenoy347@gmail.com

METHODS

Computational details: We carried out the electronic structure calculations of SnTe and *Bi-In* co-doped SnTe using Quantum ESPRESSO package.¹ Ultra-soft relativistic pseudopotentials incorporating spin orbit coupling, which considers $4d^{10}5s^25p^2$, $4d^{10}5s^25p^4$, $5d^{10}6s^26p^3$ and $4d^{10}5s^25p^1$ as valence electrons of *Sn*, *Te*, *Bi* and *In* were used. A parametrized functional of Perdew, Burke, and Erzenhoff was used to approximate the exchange-correlation energy functional with generalized gradient approximation.² We used $2 \times 2 \times 1$, 32 atom relaxed supercell of primitive rock salt SnTe structure (*Fm3m* space group symmetry) to carry out the simulations of pristine and doped configurations. We used a fine grid of $12 \times 12 \times 24$ k-mesh to sample integrations over the Brillouin zone of the supercell and X- M - Γ - Z - R high symmetry path for the electronic structure determination. An energy cutoff of 50 Ry and charge density cutoff of 400 Ry was used to truncate the wavefunctions represented by plane wave basis.

Experimental details: High purity (99.995+ %) *Sn*, *Te*, *Bi* and *In* procured from Alfa Aesar were used for synthesis without further purification. High quality crystalline ingots of $\text{Sn}_{1-3x}\text{Bi}_{2x}\text{In}_x\text{Te}$ ($x=0.0, 0.01, 0.02, 0.03$) were synthesized by mixing *Sn*, *Te*, *Bi* and *In* in appropriate ratios in carbon coated quartz tube. The tubes were flame sealed under vacuum (10^{-5} Torr) and heated slowly to 800 °C for 10 hours and then 900 °C for 10 hours and then slowly cooled down to room temperature. The product was finely ground using mortar and pestle and densified by hot pressing the pellet obtained using a graphite dye in vacuum.

We carried out powder X-ray diffraction studies using JEOL X-ray diffractometer using Cu K_α ($\lambda = 1.54178 \text{ \AA}$) radiation. Transmission electron microscope (TEM) images were obtained using Philips CM200 TEM operating with an accelerating voltage of 20-200kV with a resolution of 2.4 \AA . We determined electrical conductivity (σ) and Seebeck coefficient (S) in the

temperature range of 300 K - 840 K under helium atmosphere using ZEM -3M8 instrument. The samples were cut in parallelepiped shape ($\sim 2 \times 2 \times 8 \text{ mm}^3$) for the conductivity measurements, which were done in the longer direction. We determined the carrier concentrations using Hall coefficient measurements (PPMS system) at 300 K. The carrier concentration, n , was determined using equation $n = 1/eR_H$, where e is the electronic charge, R_H is Hall coefficient. To determine thermal conductivity, thermal diffusivity was multiplied by temperature dependent heat capacity (derived using standard sample pyroceram) and the density of the sample. The samples were cut in coin shape ($\sim 8 \text{ mm}$ diameter and $\sim 2 \text{ mm}$ thickness) for thermal diffusivity measurement using laser flash diffusivity method in the temperature range from 300 K - 840 K. The density of the pellets obtained was in the range $\sim 97 \%$ of the theoretical density. The electronic thermal conductivity was determined by using Wiedemann-Franz law $K_{el} = L\sigma T$, where L is the Lorenz number obtained by fitting Seebeck data into reduced chemical potential.

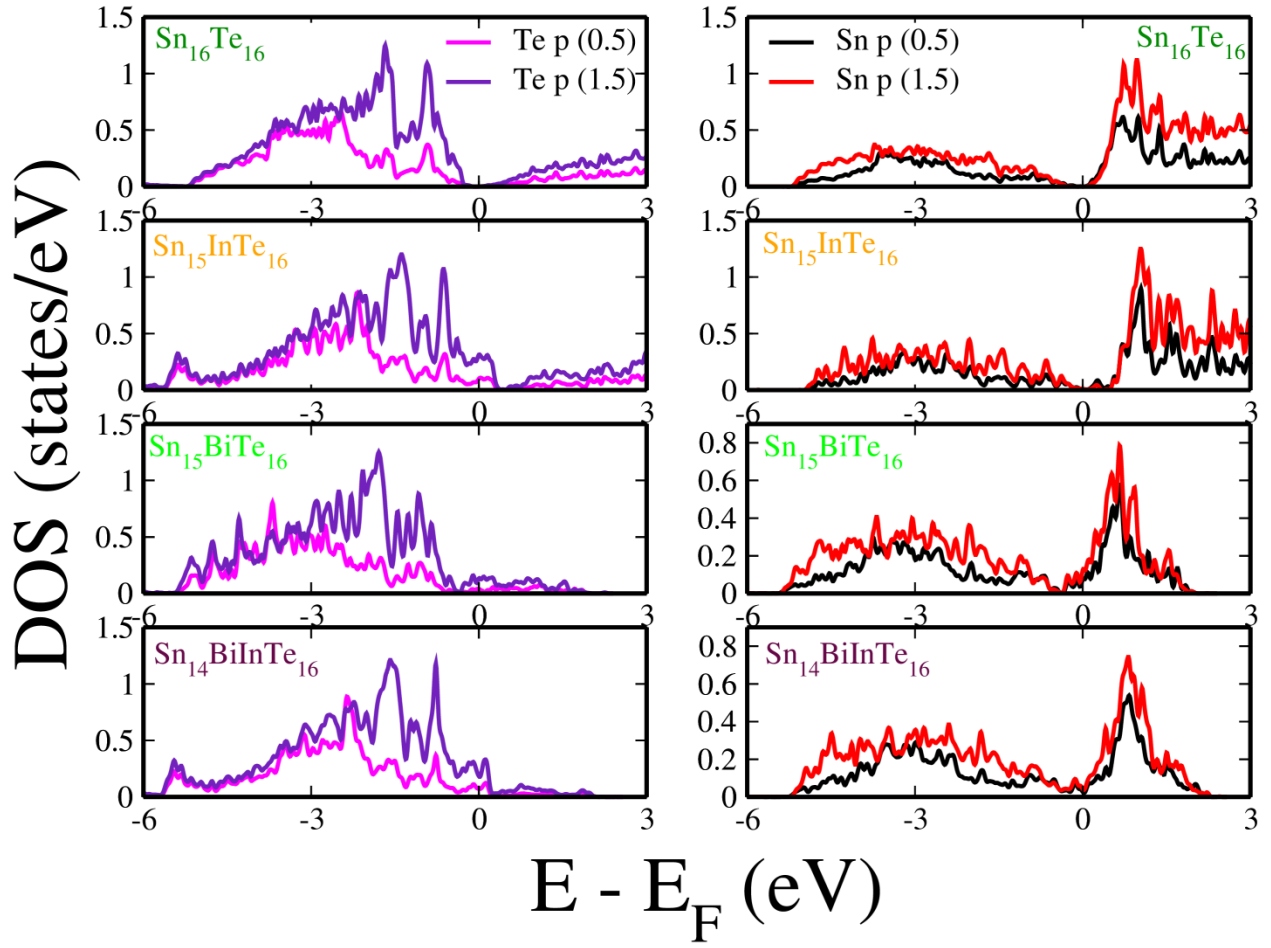


Figure S1. Partial density of states (pdos) of $\text{Sn}_{16}\text{Te}_{16}$, $\text{Sn}_{15}\text{InTe}_{16}$, $\text{Sn}_{15}\text{BiTe}_{16}$, $\text{Sn}_{14}\text{BiInTe}_{16}$ showing contribution of *Te* ‘p’ orbitals and *Sn* ‘p’ orbitals.

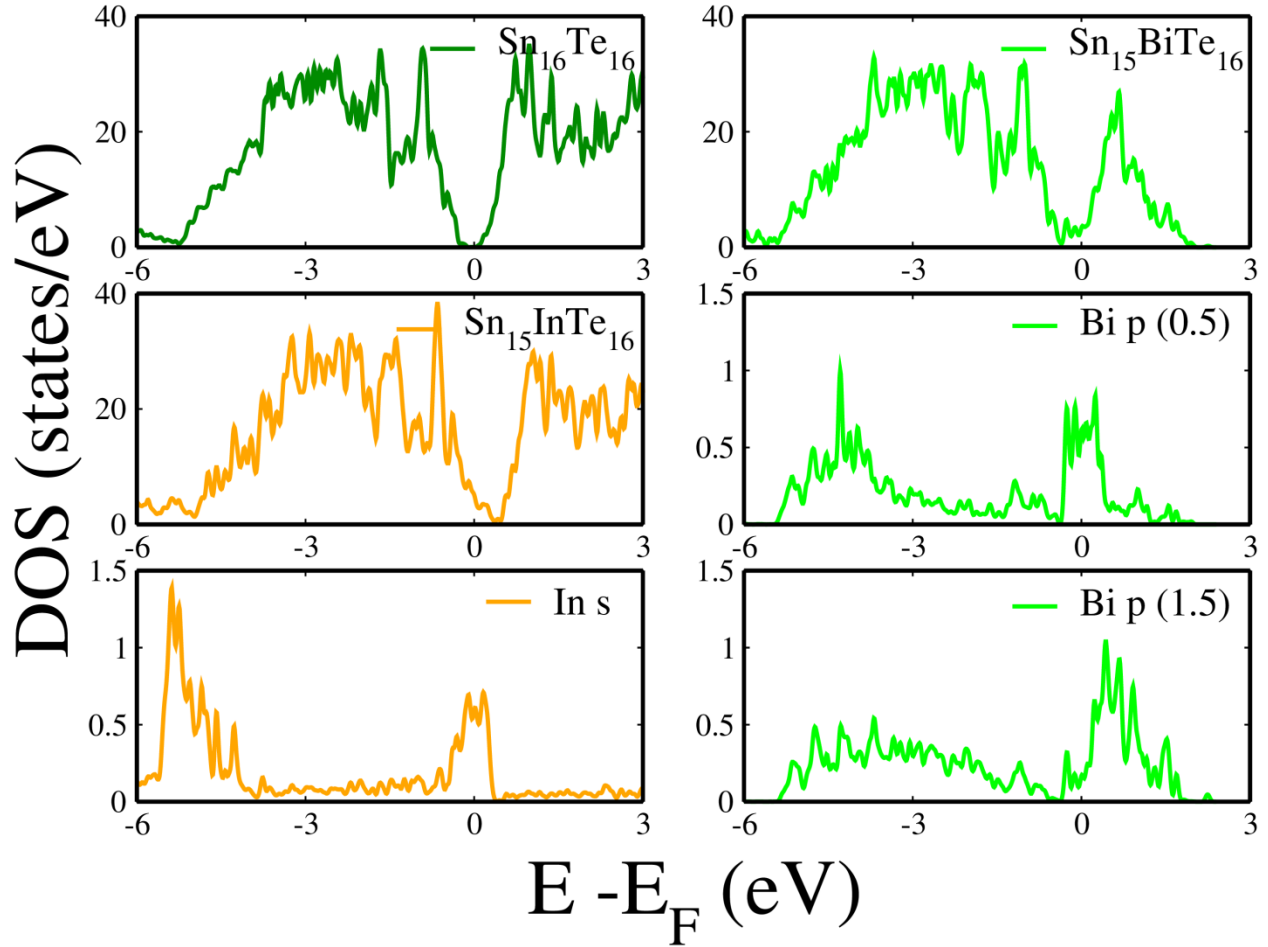


Figure S2. Total DOS and pdos of $\text{Sn}_{16}\text{Te}_{16}$, $\text{Sn}_{15}\text{BiTe}_{16}$, $\text{Sn}_{15}\text{InTe}_{16}$ showing contribution of *Bi* ‘p’ orbitals and *In* ‘s’ orbitals in *Bi* and *In* doped *SnTe*, respectively. The highest contributions from *In* and *Bi* orbitals are seen around ~ 0 eV and ~ -5.5 eV wherein *In* ‘s’ orbitals hybridize with *Te* ‘p’ orbitals and around ~ 0 eV and ~ -4.5 eV wherein *Bi* ‘p’ orbitals hybridize with *Te* ‘p’ orbitals and *Sn* ‘p’ orbitals.

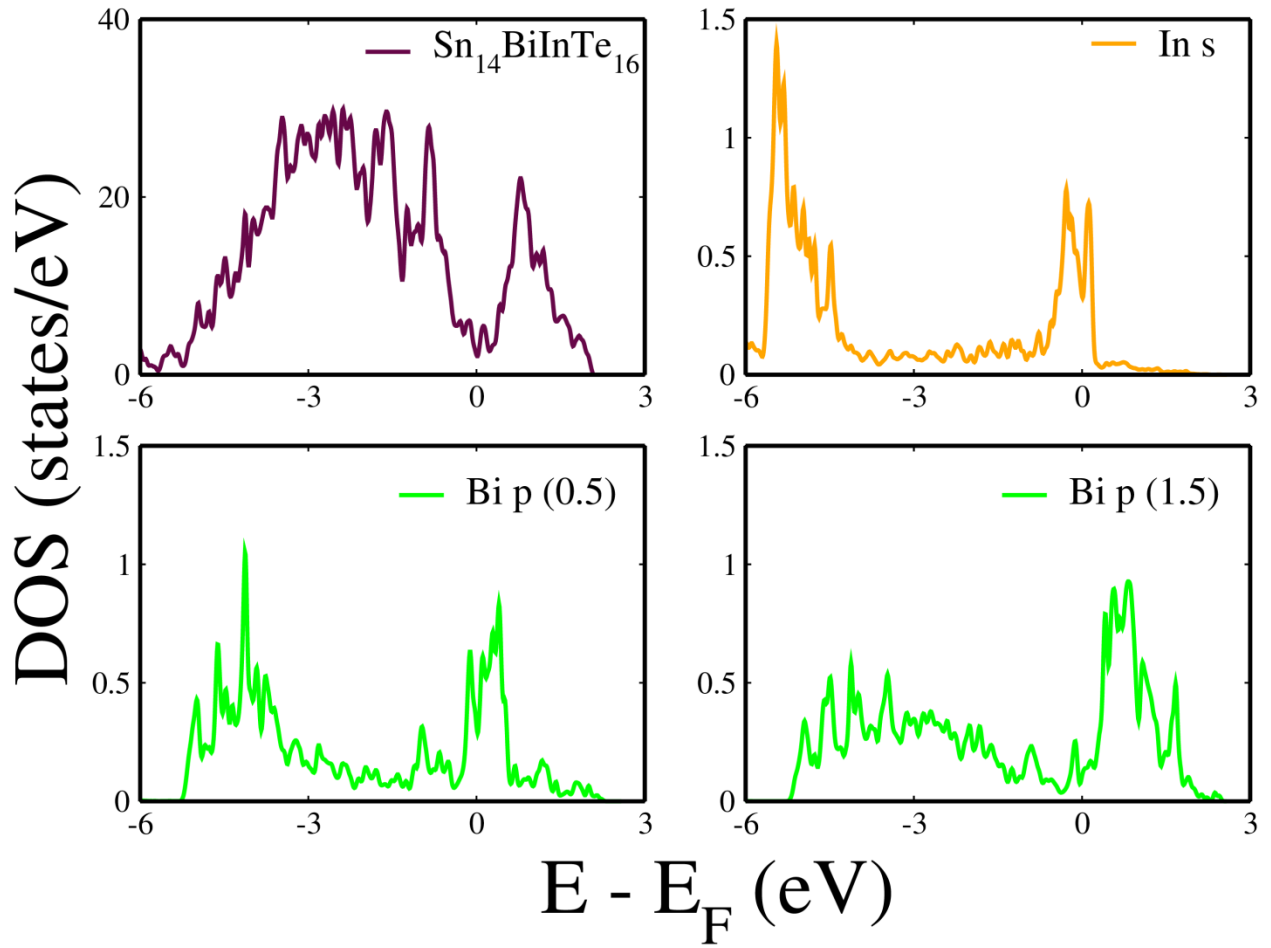


Figure S3. Total DOS and pdos of *Bi-In* co-doped SnTe showing contribution of *Bi* ‘p’ orbitals and *In* ‘s’ orbitals.

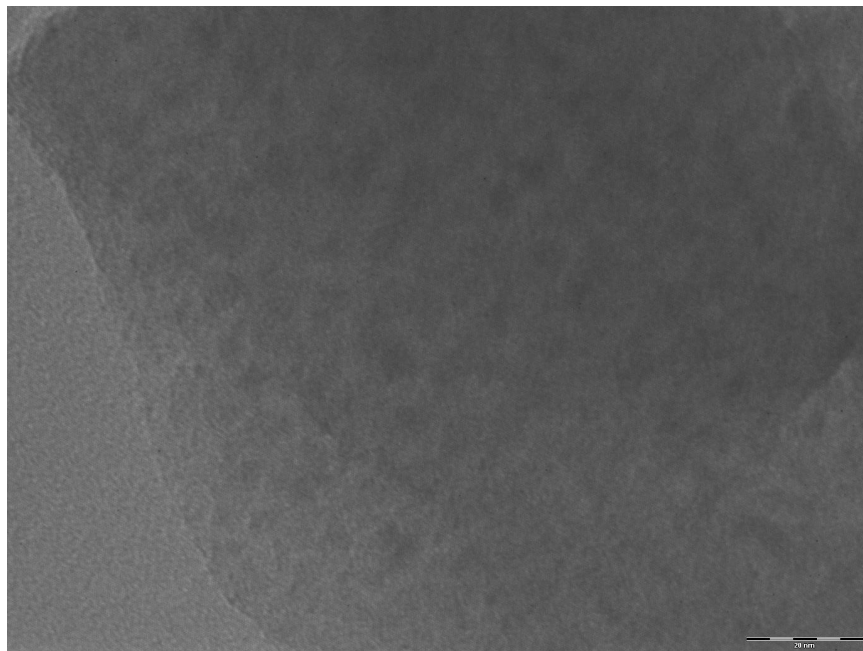


Figure S4. Low magnification TEM image of Sn_{1-3x}Bi_{2x}In_xTe sample where $x = 0.03$. The scale bar represents 20 nm. The dark spots represent the *Bi* nano-precipitates.

Table S1. Elemental percentage composition of *Bi-In* co-doped SnTe samples using EDS analysis at various area marked in TEM images of Figure 3.

Element	Percentage composition (%)		
	Spot 1	Spot 2	Spot 3
Sn	47.09	45.89	44.34
Te	49.96	50.11	50.43
Bi	1.97	2.49	3.77
In	0.98	1.51	1.46

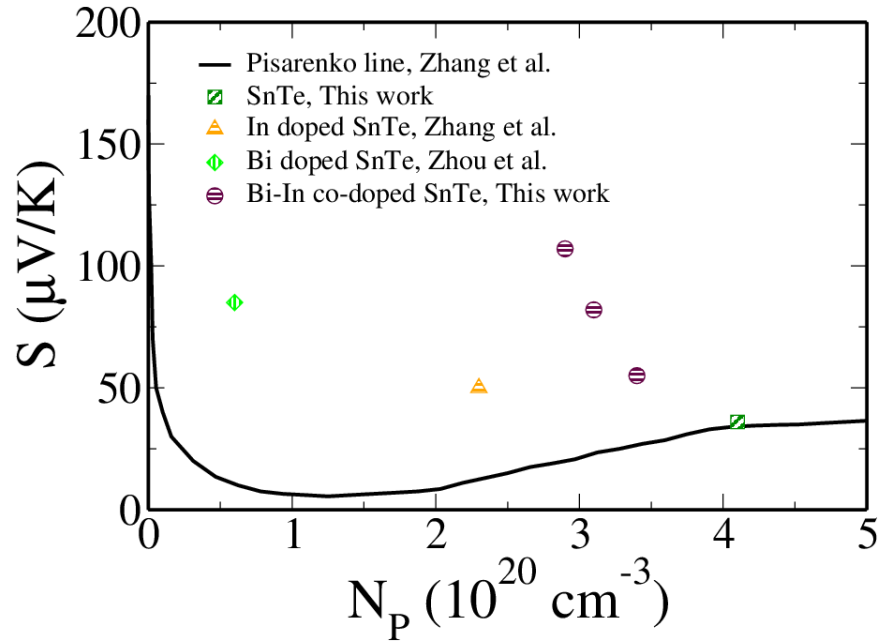


Figure S5. Room temperature Seebeck values as a function of carrier concentration N_p . The Pisarenko line is derived using two valence band model with light hole valence band having an effective mass of $0.168 m_e$ and heavy hole valence band having an effective mass of $1.92 m_e$ with the energy gap of 0.35 eV between the two sub-bands.³ For comparison with previous reports the Seebeck values of optimized concentration of *In* and *Bi* singly doped SnTe has been marked with respect to their carrier concentration.^{3,4}

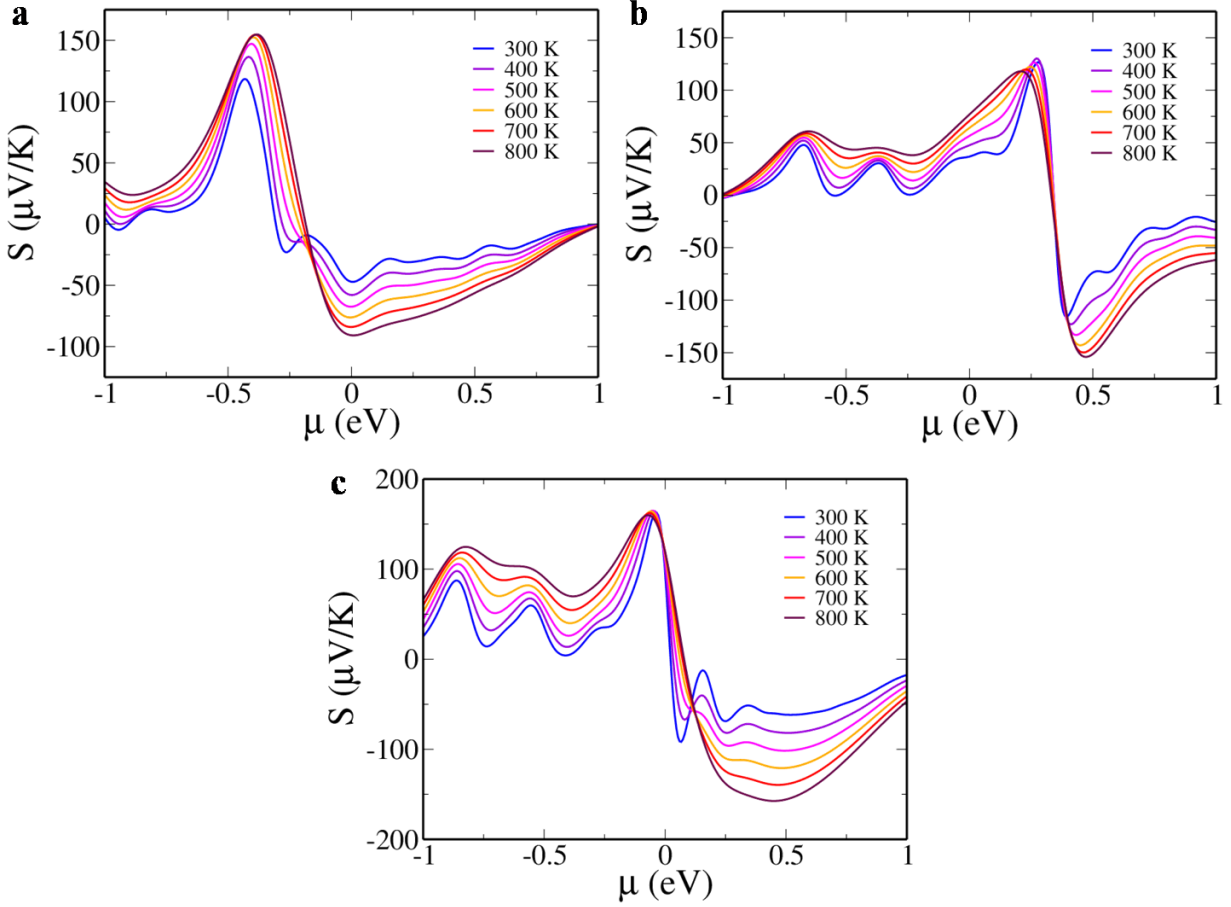


Figure S6. Seebeck values of a) $\text{Sn}_{15}\text{BiTe}_{16}$, b) $\text{Sn}_{15}\text{InTe}_{16}$, c) $\text{Sn}_{14}\text{BiInTe}_{16}$ as a function of chemical potential (μ) at various temperatures. The Fermi level is set at zero.

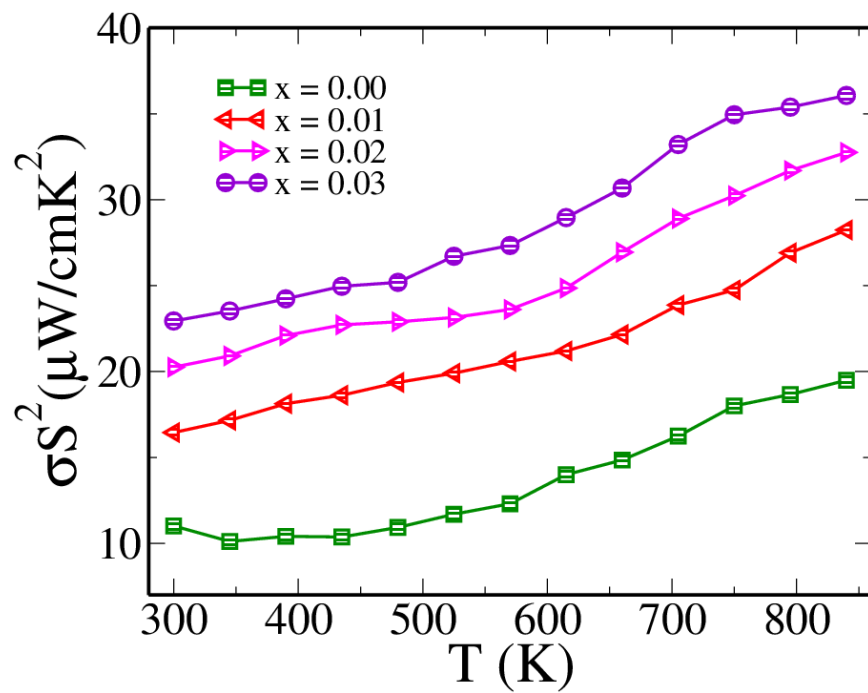


Figure S7. Variation of the power factor with the temperature for $\text{Sn}_{1-3x}\text{Bi}_{2x}\text{In}_x\text{Te}$ samples.

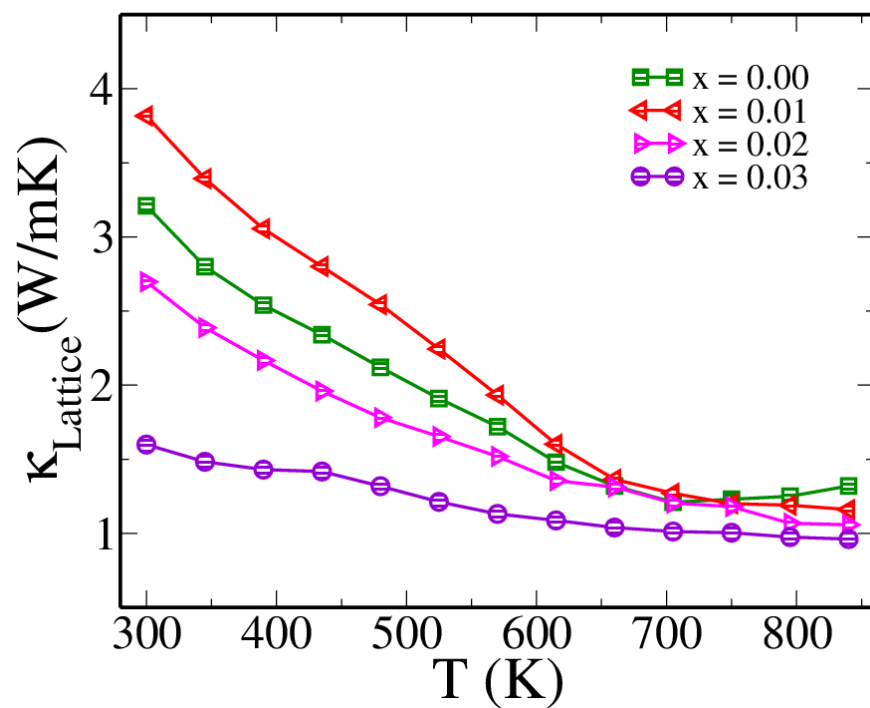


Figure S8. Variation of the lattice thermal conductivity with the temperature for $\text{Sn}_{1-3x}\text{Bi}_{2x}\text{In}_x\text{Te}$ samples.

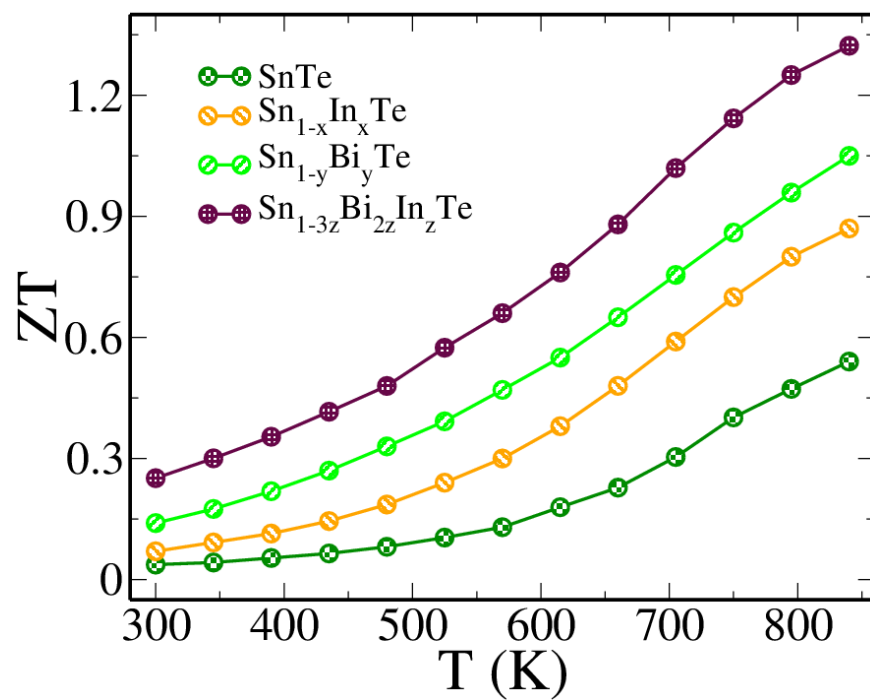


Figure S9. Comparison of ZT values pristine and doped SnTe samples at their optimized concentration where $x = 0.02$, y and $z = 0.03$.

References

1. Giannozzi, P.; Baroni, S.; Bonini, N.; Calandra, M.; Car, R.; Cavazzoni, C.; Ceresoli, D.; Chiarotti, G.L.; Cococcioni, M.; Dabo I. et al. Quantum Espresso: a Modular and Open-Source Software Project for Quantum Simulations of Materials. *J. Phys.: Condens Matter* **2009**, *21*, 395502.
2. Perdew, J. P.; Burke, K.; Ernzerhof, M. Generalized Gradient Approximation Made Simple. *Phys. Rev Lett.* **1996**, *77*, 3865-3868.
3. Zhang, Q.; Liao, B.; Lan, Y.; Lucas, K.; Liu, W.; Esfarjani, K.; Opeil, C.; Broido, D.; Chen, G.; Ren, Z. High Thermoelectric Performance by Resonant Dopant Indium in Nanostructured SnTe. *Proc. Natl. Acad. Sci. U.S.A.* **2013**, *110*, 13261-13266.
4. Zhou, Z.; Yang, J.; Jiang, Q.; Luo, Y.; Zhang, D.; Ren, Y.; He, X.; Xin, J. Multiple effects of Bi doping in enhancing the thermoelectric properties of SnTe. *J. Mater. Chem. A* **2016**, *4*, 13171-13175.